Marine Pollution Bulletin 154 (2020) 111037

Contents lists available at ScienceDirect

Marine Pollution Bulletin

journal homepage: www.elsevier.com/locate/marpolbul

Minimum drift times infer trajectories of ghost nets found in the Maldives

Martin Stelfox[a,b,*], Christophe Lett[c], Geraldine Reid[d], Graham Souch[a], Michael Sweet[a,b]

[a] Aquatic Research Facility, Environment Sustainability Research Centre, College of Life and Natural Sciences, University of Derby, UK
[b] Olive Ridley Project, 11 Dane Close, Bramhall, Stockport, Cheshire SK7 3LF, UK
[c] MARBEC, IRD, Ifremer, Univ Montpellier, CNRS, Sète, France
[d] Botany, National Museums Liverpool, William Brown Street, Liverpool L3 8EN, UK

ARTICLE INFO

Keywords:
Ghost nets
Lagrangian
Purse seine
Gill nets
Biofouling
Drift trajectories
Plastisphere
Plastics
Pollution

ABSTRACT

This study explores methods to estimate minimum drift times of ghost nets found in the Maldives with the aim of identifying a putative origin. We highlight that percentage cover of biofouling organisms and capitulum length of *Lepas anatifera* are two methods that provide these estimates. Eight ghost nets were collected in the Maldives and estimated drift times ranged between 7.5 and 101 days. Additionally, Lagrangian simulations identified drift trajectories of 326 historical ghost nets records. Purse seine fisheries (associated with Korea, Mauritius, the Philippines, Spain, France and Seychelles) and gill nets from Sri Lanka were identified as 'high risk' fisheries with regard to likley origins of ghost nets drifting into the Maldives. These fisheries are active in areas where dense particle clusters occured (drift trajectories between 30 and 120 days). Interestingly, ghost nets drifting less than 30 days however, remained inside the exclusive economic zone of the Maldivian archipelago highlighting potential illegal, unreported and unregulated fishing activity is occuring in this area. This study therefore points to the urgent need for gear loss reporting to be undertaken, especially by purse seine and gill net fisheries in order to ascertain the source of this major threat to marine life. This should also be coupled with an improvment in the data focused on spatial distribution of the abandoned, lost or discarded fishing gear originating from both large- and small-scale fisheries.

1. Introduction

Abandoned, lost or discarded fishing gear (ALDFG) also known as 'ghost gear' has been widely recognised as one of the most important components of debris in our oceans (Watters et al., 2010; Hardesty et al., 2015; Stelfox et al., 2016; Wilcox et al., 2016; Consoli et al., 2018; Miller et al., 2018). Historically, the majority of fishing gear was made from natural materials such as cotton, coconut or hemp. Therefore, they would have had a relatively short lifespan even when lost or abandoned. However, starting in the late 1940s and, early 50s these materials were replaced with synthetics, extending their lifetime substantially (Von Brandt, 1984). Now, when nets are abandoned, lost or discarded they often become locked in ocean gyres or travel great distances, crossing political borders before eventually becoming stranded or found in nearshore habitats like coastal coral reefs (Matsuoka et al., 2005; Stelfox et al., 2015). Management decisions on this issue are often challenging as 'ownership' of the gear is often unknown and difficult to backtrack.

Large quantities of ghost gear have been reported in the Maldivian archipelago (Stelfox et al., 2015, 2019), despite commercial application of pole and line for catching tuna and subsistence hand line methods dominating the fisheries in the Indian Ocean island state (Adam et al., 2015). Understanding where ALDFG are coming from would be a first step to tackling the issue and reducing the threats to marine life. To date, broad classifications of the possible fisheries responsible have been identified by statistically modelling ghost net characteristics and attempting to assign them to a specific fishery (Wilcox et al., 2013; Stelfox et al., 2019). However, aging the floating nets to provide time adrift, and analysing drifting trajectories using ocean current simulations in combination with the spatial distribution of fisheries should bring us closer to identifying their origins.

There are a number of ways one can monitor and/or obtain drift times for floating debris. For example, the assessment of fouling organisms on debris (Hellio et al., 2004; Banerjee et al., 2011; Callow and Callow, 2011; Kiessling et al., 2015; Fazey and Ryan, 2016). Typically, active fishing gear is cleaned between trips, effectively minimising damage and increasing longevity and catch efficiency (Pers. Obs.). Biological growth on the surface of nets would thereby act as a 'biological clock' indicating how long they have been in the water since they were last cleaned. Indeed, the succession of certain species or taxa

* Corresponding author at: Aquatic Research Facility, Environment Sustainability Research Centre, College of Life and Natural Sciences, University of Derby, UK.
E-mail address: martin@oliveridleyproject.org (M. Stelfox).

https://doi.org/10.1016/j.marpolbul.2020.111037
Received 28 October 2019; Received in revised form 1 March 2020; Accepted 1 March 2020
Available online 07 March 2020
0025-326X/

and their respective growth rates have been shown to age other types of marine debris (Ye and Andrady, 1991). In particular, diatoms and barnacles may be useful indicator groups to assess drift as they are prevalent across all oceans and are major biofouling organisms on all types of litter including nets (Saldanha et al., 2003; Magni et al., 2015). The majority of research has, to date, focused on ways of removing biofouling or preventing settlement in the first instance (Hellio et al., 2004; Banerjee et al., 2011; Callow and Callow, 2011). This is because biofouling can reduce efficiency on floating wave energy devices (Nall et al., 2017), block water intake pipes (Rajagopal and Jenner, 2012) for example, as well as adding weight to fixed structures (Shi et al., 2012), and increasing drag and subsequent fuel consumption in marine vessels (Schultz, 2007).

Another approach commonly utilised to predict the origin of marine litter (e.g. plastics) is the use of ocean current data (Lebreton et al., 2012; Maximenko et al., 2012; Liubartseva et al., 2016; Guerrini et al., 2019; Jalón-Rojas et al., 2019). The Maldives again provides an interesting case study as the country lies north south perpendicular to an east west current system (Shankar et al., 2002). However, ocean circulation is complex, and currents vary not only seasonally, but in response to short term events like tropical cyclones and between years depending on pan-tropical atmospheric-ocean forcing. This latter aspect is related to phenomena like the El Niño Southern Oscillation and the Indian Ocean Dipole (Schott et al., 2009). This means broad generalisation is not always appropriate when analysing the dispersal of objects (Wood et al., 2016).

In this study, we attempted to assess the origin of ghost gear found within the Maldivian archipelago using a multipronged approach. First, we experimentally deployed nets to quantify the development and growth rates of biofouling organisms in order to estimate time adrift. Measurements included diatom population and taxonomy and percentage cover of all fouling organisms. Additionally, we deployed surface buoys to analyse growth rates of a common biofouling organism, the pelagic gooseneck barnacle (*Lepas anatifera*). Secondly, we applied these age estimate techniques to eight ghost nets found floating in the Maldives and backtracked the nets (based on these age estimates) using a Lagrangian model to find their putative origin. Here, we also utilised a historical and much larger dataset of 326 recovered ghost nets (each with reported times and locations of recovery in Maldivian waters but without estimates of their drift durations) to explore which other fisheries may be responsible for these 'lost' nets. To do this, we utilised Lagrangian modelling to backtrack their putative origin using several plausible values of drift duration (10, 30, 60, 90 and 120 days).

2. Methods and materials

2.1. Study site

The Maldivian archipelago consists of 26 atolls stretching across almost 1 million square km (Adam, 2006). Geographically, the Maldives is enclosed along its northern border and lies north-south across an east-west monsoonal current system (Shankar et al. 2004, Supplementary material S1a). Variation in sea surface temperature (SST) is very small in the Maldives typically ranging between 28.27 and 29.38 °C (Alonso-Garcia et al., 2019). However, in this study SST ranged between 28 and 31 °C.

All experiments were conducted inside an atoll lagoon in shallow coastal waters, 18 m deep and 20 m away from the sloping reef (Supplementary material S1b). In contrast ghost net fragments were collected opportunistically from the ocean surface from inside island atolls (lagoons) or from outside the atoll chain in deeper oceanic water (Supplementary material S2b–e). Atoll lagoons in the Maldives vary in depth from 30 m to 50 m (Fritz et al., 2006) and are typically calmer more sheltered waters than deeper oceanic waters. The Maldives is subject to two major monsoonal patterns that bring with it opposing ocean surface currents. During the northeast (NE) monsoon, surface currents approaching the islands originate from the Bay of Bengal, whereas during the southwest (SW) monsoon they approach from the Arabian Sea (Shankar et al. 2004). Typically, floating debris, including ghost nets from neighbouring countries get trapped by the island chain. This gives researchers the unique opportunity to remove and analyse this debris to determine drift trajectories and putative origin.

2.2. Experimental assessment of bioaccumulation on floating nets and buoys

Diatom diversity and biofouling percentage cover were assessed on newly deployed, high-density polypropylene (HDPP), multifilament fishing nets (supplied by Garware Wall Ropes Ltd). This study was conducted at the Dhuni Kholu resort, in Baa atoll, Maldives (5° 2′27.17″N, 72°53′4.01″E). A single net was divided into three separate replicate fragments (100 cm × 100 cm size). Two fishing buoys were attached to the sea floor, 18 m above and 20 m away from the sloping reef. The two buoys were fixed by a further rope on the surface (Supplementary material S1f,a). The nets were attached to the line with zip ties that were first coated with antifouling paint to minimise cross contamination. Each repeat (net) was arranged so that no direct contact could be made between replicates (Supplementary material S1f,b). The nets were sub-sampled (ensuring the knot and twine either side was included - Supplementary material S2) on day two, four, six, eight and ten, then every two weeks thereafter up until 112 days.

Samples were placed immediately in 2.5% glutaraldehyde and stored in a fridge until further sample preparation and analysis. Samples were then dehydrated via a series of 60, 75, 85, 95 and 100% absolute ethanol for 15 min each, with final dehydration consisting of air drying for 1 h. Specimens were then mounted on an aluminium stub with Achesons Silver Dag (dried overnight) and coated with gold (standard 15 nm) using an Emi Tech K550X Splutter Coating Unit. Specimens were then examined using a Stereoscan 240 scanning electron microscope, and digital images collected by Orion 6.60.6 software. Scanning electron micrographs (at a magnification of 1500 X) were taken along a 0.1 mm^2 transect in the middle of the twine and 0.1 mm^2 transect along the centre of the knot. We assessed each micrograph for diatoms, which were identified to the lowest taxonomic or morphological level. Diatoms that fell outside the transect frame or not attached to the net itself (i.e. likely associated with the surrounding water column) were excluded from the analyses. Moreover, diatoms that could not be identified due to partial loss of structure were also excluded. We then calculated commonly used diversity indices such as species richness (S – total number of different species within the transect frame), total abundance, Shannon-Wiener diversity index (H, Weaver and Shannon, 1949), Simpson index (D, Simpson, 1949) and the Pielou evenness index (J, Pielou, 1966). These indices allowed us to explore species rarity, abundance and distribution for each time interval to identify patterns over time. We also opportunistically recorded additional organisms of note, in order to capture any successional changes of other biota communities over time. However, these were excluded from diversity analyses due to the difficulty in distinguishing between background noise (which may include filamentous algae, mucilage, encrusting communities and/or the high abundance of bacteria that would skew diversity indices for example). That said, we did combine diatom and other opportunistically recorded organism counts to perform a Z score hierarchical clustering using Euclidean distance measure. Here each row (organism or species) was scaled before analyses using heatmap.2 function in gplot (Warnes et al., 2015). This allowed for a visual representation of community succession.

Alongside diversity indices, percentage cover of all biota growing on the surface of the net was calculated. To do this, three scanning electron micrographs along each transect (as mentioned above) were imaged to give a 0.03 mm^2 surface area per micrograph (six micrographs per sample, knot and twine). Images were then inputted into the digital imaging software, Image J (Schneider et al., 2012). The threshold of each micrograph was manually adjusted until attached biota was

highlighted in red to estimate percentage cover. In rare cases, salt crystals were present on the surface. However, these were excluded from all analyses and we assumed no growth was occurring under the crystal. Due to contrast and brightness variations in some images not all of the biota was captured by the threshold adjustments and in some instances, threshold only captured a small proportion of the visible surface growth. In such cases, the paintbrush tool was used to manually highlight the cover.

The growth rate of gooseneck barnacles (*Lepas anatifera*) was measured in a separate experiment at the Bodu Hithi resort, North Male atoll, Maldives (4°25′41.18″N, 73°23′7.70″E). Three surface buoys, on a fixed line 20 m away from the sloping reef, 18 m above the sea floor were deployed. When biofouling had occurred, 27 gooseneck barnacles (9 for each of the three replicates/buoys) were randomly selected and their growth rates calculated. The capitulum length was measured (in mm) from the apex to base with a ruler (Supplementary material S3). In addition, digital images were also taken when possible in order to obtain more accurate sizes using image J digital software (Schneider et al., 2012). Measurements were taken once every seven days for a total of 105 days.

We used the Shapiro-Wilk test (Shapiro and Wilk, 1972) to check for normality within our barnacle and percentage cover data. After rejecting the null hypothesis (H_o normally distributed data) in both experiments we performed the non-parametric Kruskal-Wallis test (Kruskal and Wallis, 1952) to check for significant difference in growth rates between the buoys (barnacle experiment) and percentage cover between the nets (percentage cover experiment). After this we fitted linear and polynomial regression trend lines and selected the best fit according to the highest adjusted R squared value. All analyses were conducted in the statistical programming language R vs 3.4.2 (R Core Team, 2018).

2.3. Ghost net data

Drifting ghost nets were collected opportunistically by biologists on board a turtle expedition conducted by the Olive Ridley Project on two separate occasions; November 2017 and February 2019. In 2017 independent nets ($n = 5$) were immediately stored in 2.5% glutaraldehyde, while due to limitations in the field in 2019 samples could not be fixed on site and only nets found with barnacles were recorded ($n = 3$). We applied the analyses detailed above to estimate drift times of these nets.

Further, stranded ghost nets occurring in Maldivian waters have been recorded by the Olive Ridley Project between 2013 and 2018. In this timeframe 326 nets have been found ($n = 149$ from the NE monsoon and $n = 177$ from the SW monsoon) with reported times and locations of recovery but not their age. All nets reported were of twisted construction and made from high density polypropylene (HDPP).

2.4. Lagrangian modelling

To explore where ghost nets found within the Maldives may have come from, we used the final net location to backtrack possible origins. This was done using the offline Lagrangian particle dispersal model Ichthyop (Lett et al., 2008; http://www.ichthyop.org/). Diffusion was activated following guidelines by Peliz et al. (2007). Advection was accounted for using 2D hydrodynamic data from Ocean Surface Current Analysis Real-time (OSCAR, Lagerloef et al., 1999; http://www.oscar.noaa.gov). OSCAR is a global current product derived from remote-sensing data and provided on a 1/3° grid with a 5-day resolution. It was evaluated in the tropical Indian Ocean by Sikhakolli et al. (2013).

We initially released 1000 'particles' at the same time and location as each of the 326 ghost nets found (326,000 particles in total). For the eight age estimated nets we released a further 10,000 particles each (80,000 particles in total). For these nets we used the estimated drift times to set the duration of the simulated backwards drift. For the 326 unaged nets (i.e. those without any prior knowledge of their drift times) we ran the models backwards in time for 10, 30, 60, 90 and 120 days. Plots were generated to illustrate the number of 'particles' per 1/4° squares for both 326 ghost nets and eight ghost net samples.

2.5. Fishery interaction

Data were utilised on the spatial distribution of operating fisheries reported to the Indian Ocean Tuna Commission (IOTC) at a 1° x 1° grid cell resolution to overlay fishing grounds onto our simulations of net origin. To do this, the grid codes from the Coordinating Working Party (CWP) of the Food and Agriculture Organisation (FAO) were converted into latitude and longitude coordinates by finding the centroid of each statistical grid. These were then layered onto the 'particle' distribution plots in QGIS (V. 3.4) to highlight fishery activities.

Data and analyses (barnacle growth, percentage cover and ghost net location) was uploaded to the Olive Ridley Project website and is available for download at https://oliveridleyproject.org/download-minimum-drift-time-data.

3. Results

3.1. Experimental assessment of bioaccumulation on floating nets and buoys

Fifteen morphologically distinct diatoms were identified attached to the experimentally deployed nets at Baa Atoll, in the Maldives. These included two asymmetrical biraphid species from the genus *Amphora* (Fig. 3.1a,b), six monoraphid species (*Anorthoneis eurystoma*, two *Cocconeis* sp., *Achnanthes pseudobliqua*, *Achnanthes* sp., and *Fragilariopsis rhombica*; Fig. 1c–h). *Nitzschia longissima* (Fig. 3.1i) was also found, along with three symmetrical biraphid species (*Gyrosigma tenuissimum*, *Parlibellus delognei*, and *Delphineis* sp.; Fig. 1j–l), a *Hyalosira* sp.; (Fig. 1m), a *Licmophora* sp.; (Fig. 1n) and *Gomphonemopsis exigua* (Fig. 1o). Many diatoms were lying flat on the nets (i.e. valve or girdle face in contact with the net, both adnate and motile diatoms). However, some were observed to be erect and attached by peduncle or stalks. The genus *Amphora* was by far the most frequently recorded (65.6%), followed by the two *Cocconeis* spp. (8.9%), the *Licmophora* sp. (6.9%), the *Hyalosira* sp. (4.1%) and *Anorthoneis eurystoma* (2.9%). The remaining observed organisms (*Achnanthes pseudobliqua*, *Achnanthes* sp. *Fragilariopsis rhombica*, *Nitzschia longissimi*, *Gyrosigma tenuissimum*, *Parlibellus delognei*, *Delphineis* sp. and *Gomphonemopsis exigua*) accounted for < 1% of total abundance. It should be noted that these may be an underestimation of the true abundance of diatoms species present as some were positioned on the net showing only their girdle so could not be identified from this orientation (11.5%).

Unsurprisingly a large number of bacteria (Cocci shaped) appear on nets in the Maldives within 4 days and rapidly begin to colonise the surface; in terms of number of individuals they are the most abundant fouling organisms (Fig. 2a). We also observed something encrusting at the same time, but this was not discernible under the scanning electron microscope. Other organisms including amoeboid protists (Foraminifera) such as an *Elphidium* sp., (Fig. 2b) and a *Foraminifera* sp. (Fig. 2c) which started to colonise after 42 days and would likely be actively feeding on the diatoms. There were also several unidentified invertebrates, which were observed after 42 days. These included an isopod (Fig. 2d), an unknown invertebrate (Fig. 2e) and a bivalve (Fig. 2f).

After 56 days, each net was densely covered in unidentifiable fouling organisms or attached detritus, effectively obstructing the view of any diatoms if indeed present. Therefore, we truncated diversity analyses for the first 56 days only, and it is suggested that this method for aging nets would only be suitable for the first couple of months at best. Overall, species richness and abundance steadily increased for the first 10 days, reflecting the fast colonisation of a newly introduced ecological niche (Fig. 3a,b, Supplementary material S4) and early

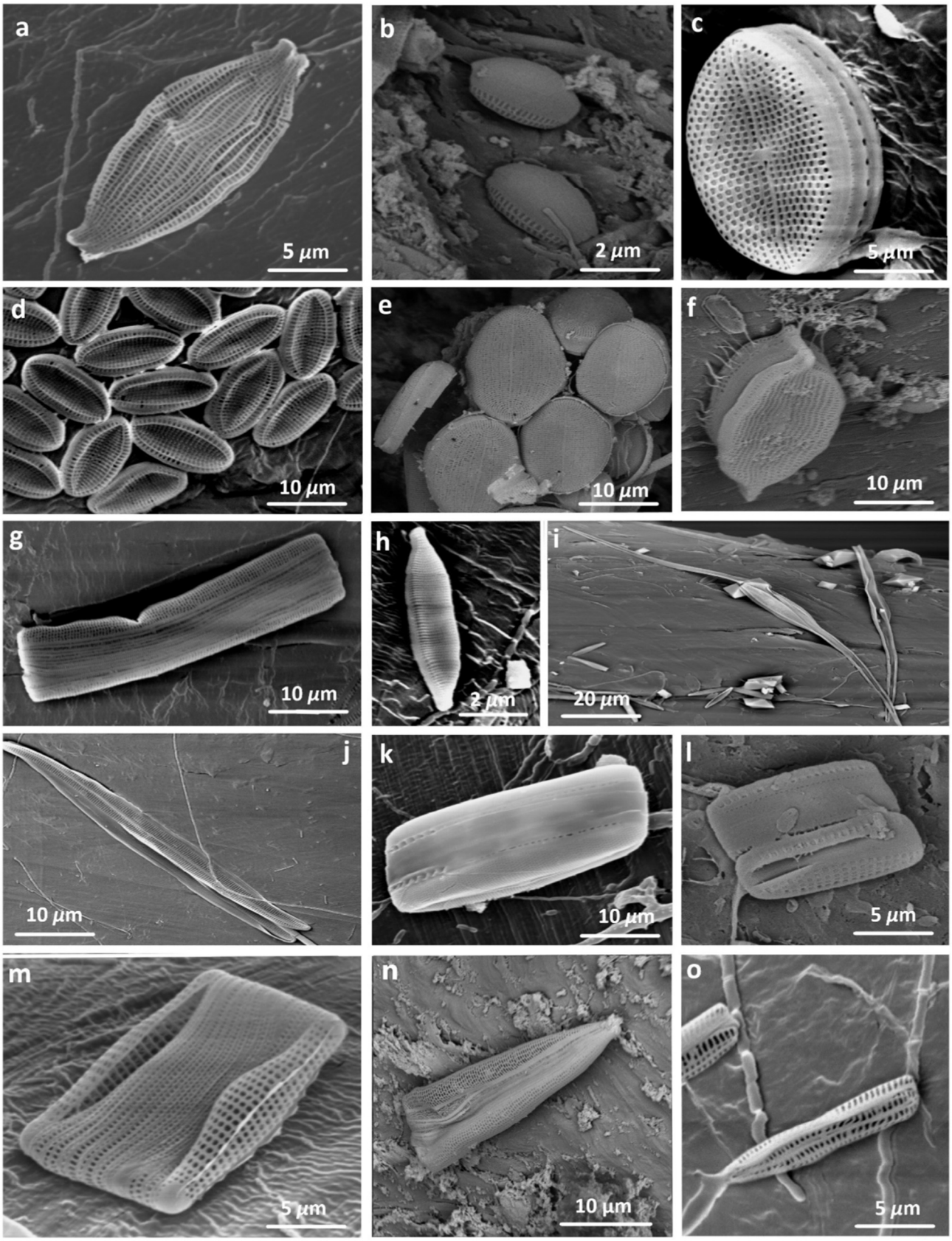

Fig. 1. Diatoms found attached to the surface of fishing nets, a: *Amphora* sp. *A*; b: *Amphora* sp. *B*; c: *Anorthoneis eurystoma*; *d*: *Cocconeis* sp. *A*; e: *Cocconeis* sp. *B*; f: *Achnanthes pseudobliqua*; g: *Achnanthes* sp.; h: *Fragilariopsis rhombica*; i: *Nitzschia longissimi*; j: *Gyrosigma tenuissimum*; k: *Parlibellus delognei*; l: *Delphineis* sp.; m: *Hyalosira* sp.; n: *Licmophora* sp.; o: *Gomphonemopsis exigua*.

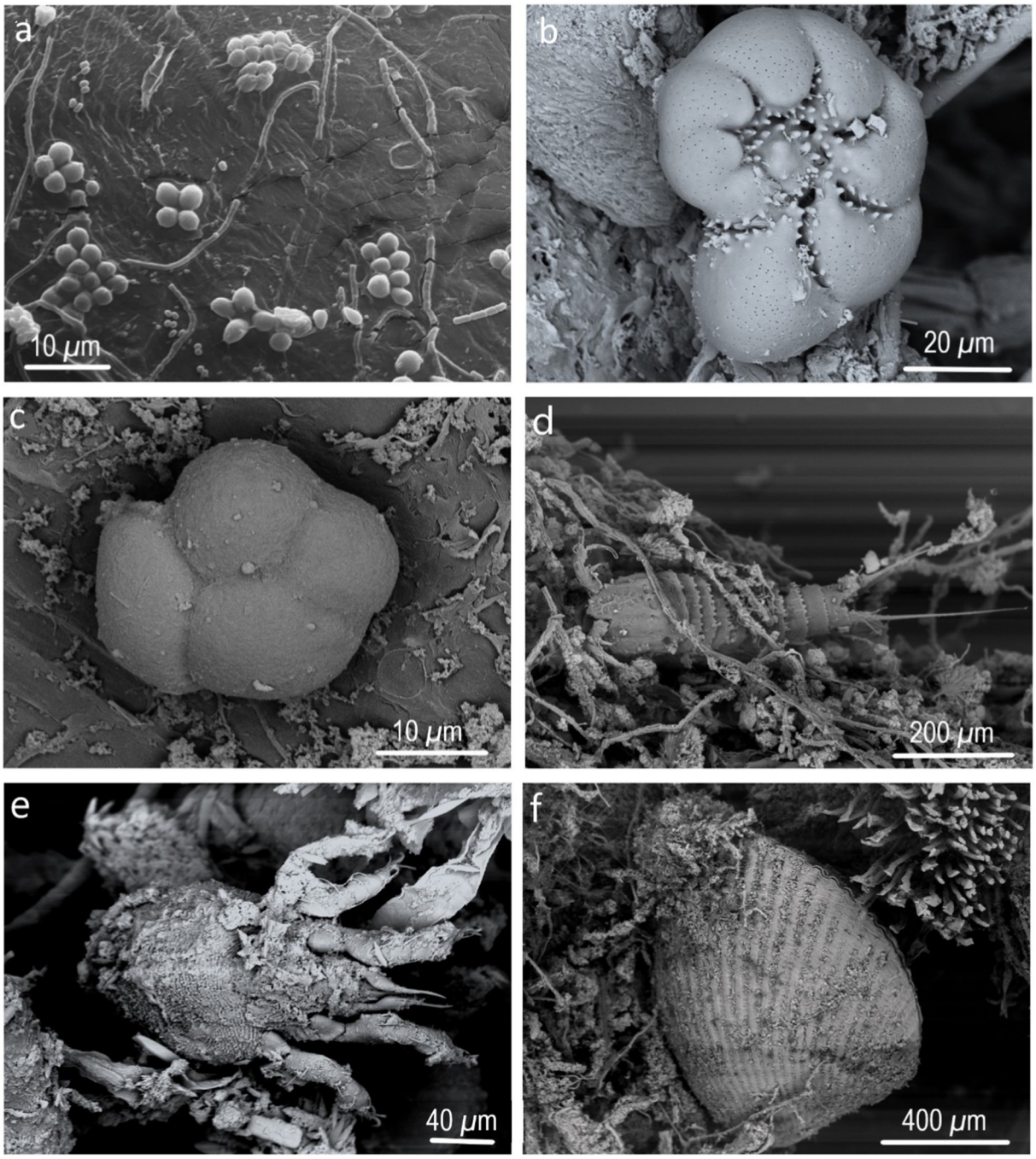

Fig. 2. Rounded cells, Foraminifera and unknown crustaceans and invertebrates found on experimental nets exposed to seawater. a: bacteria (Cocci); b: *Elphidium* sp.; c: *Foraminifera* sp.; d: unidentified *isopod* sp.; e: unknown invertebrate; f: unknown bivalve.

dominance by *Amphora* spp. (Fig. 1a, Supplementary material S4). Interestingly, after day 14, diatom diversity decreased (Fig. 3c,d), but certain species such as *Amphora* sp. (B) and *Licmophora* sp. occurred at this time and were dominant (Supplementary material S4, Fig. 1b,n). The observed decline in diatom diversity is also reflected in a decrease in evenness (Fig. 3e). Although not included in the diversity analyses, the heatmap (Supplementary material S4) also highlights that after 14 days, round shaped (*Cocci*) bacteria (Fig. 2a) peak in abundance and then become difficult to record as percentage cover of biofouling communities increases. Similarly, *Foraminifera* (Fig. 2b,c) and various unidentified invertebrates (Fig. 2d–f) first start appearing around 42 days and then dominate as percentage cover of biofouling communities increases, again making it difficult to record the presence and indeed attachment of diatoms to the nets.

Broadly, the diversity indices illustrate a stochastic relationship between the replicates associated with this study. In contrast, percentage cover of biofouling communities and average capitulum size of the pelagic gooseneck barnacle, *L. anatifera* (Fig. 3f,g), shows less variation between replicates. Up to 60 days (when percentage cover reaches near 100%), a positive linear relationship occurred (R^2 = 0.99) (Fig. 4a). Fitted linear regression models show that the expected (predicted) values match closely with actual values with small confidence intervals (Fig. 4b).

L. anatifera started to appear on the buoys between seven and 14 days after deployment. The largest individual barnacle measured 35 mm in capitulum length (maximum average 27.9 mm) at the end of

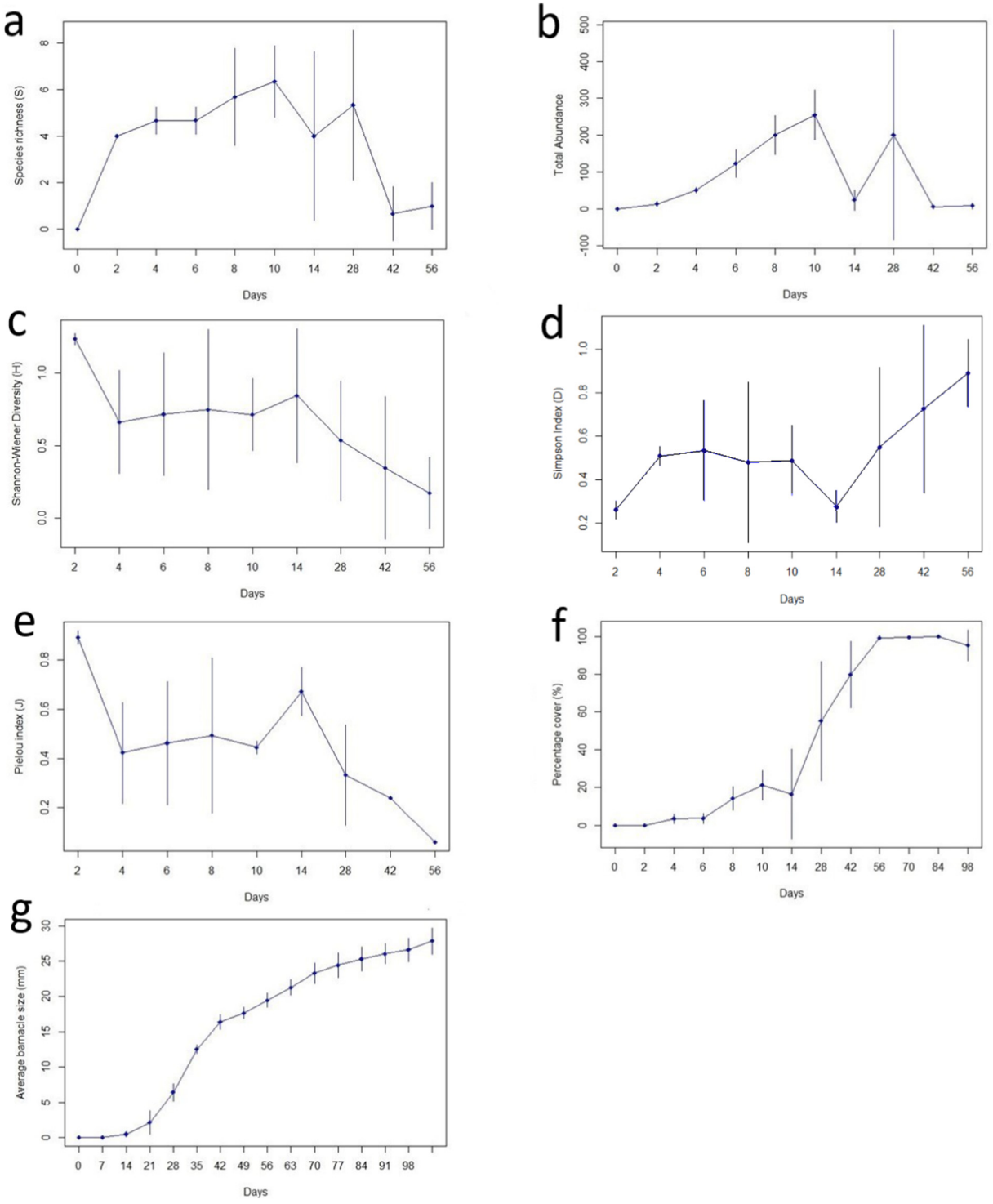

Fig. 3. Mapping variations over time against species richness (a), total abundance (b), Shannon-Wiener diversity (c), Simpson index (d), Pielou index (e), percentage cover of biofouling communities (f) and average capitulum size (mm) of *Lepas anatifera* (g). Error bars equate to standard deviations.

the experiment (105 days). Growth appeared to slow down as barnacle shell size approached the maximum average size (27.9 mm). A clear sigmoidal curve was observed for the first 105 days when an average of all barnacle sizes was taken for each time interval. A polynomial 4th order trend line (Fig. 4c) was the best fit for average *L. anatifera* capitulum size (R^2 = 0.99). The expected values match closely with actual values and partial residuals show little variance (Fig. 4d).

3.2. Ghost net age estimates and their putative origin

We analysed percentage cover of biofouling organisms and capitulum length of gooseneck barnacles to estimate minimum drift times of eight ghost nets found in the Maldives (Table 1). We applied these two methods as they illustrate clear trends and had little variance between replicates in the controlled experiments. We were able to confirm the species of barnacle growing on each net through genetic analyses and all were *Lepas anatifera*. Although we did not explore diatom diversity,

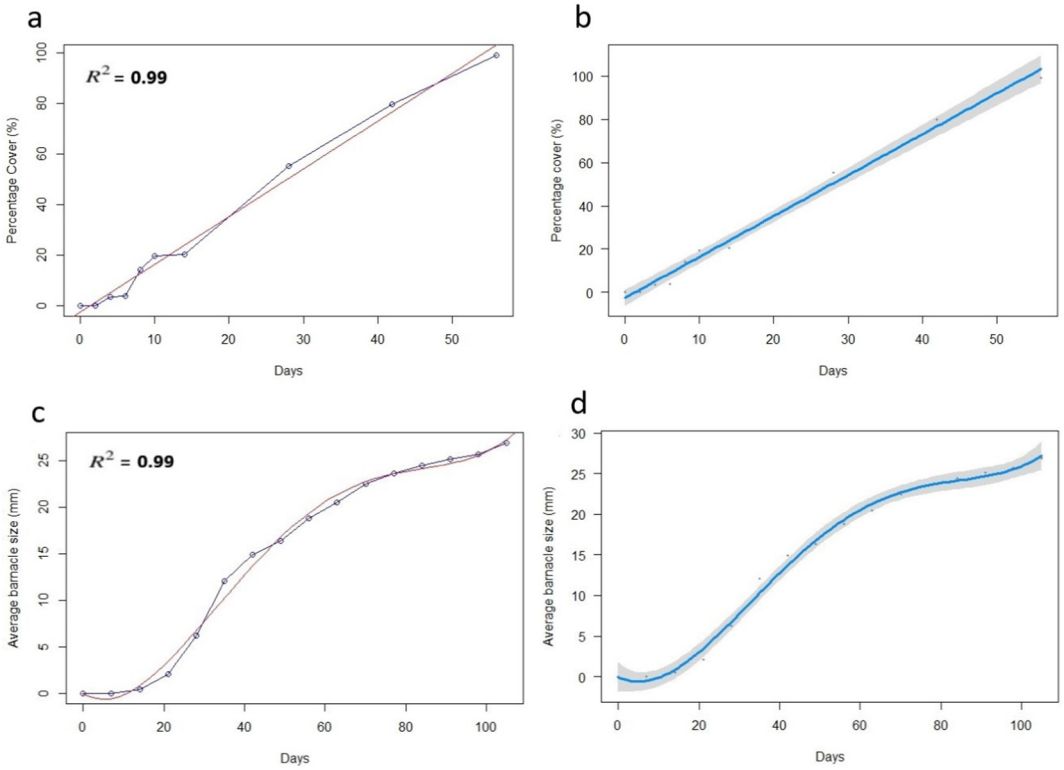

Fig. 4. (a) Biofouling communtieis can be used to assess age of ghost nets. Linear relationship between number of days and percentage cover of biofouling communities. 100% cover is reached at 56 days; so the trend is shown from 0 - 56 days. (b) Shows the expected value (blue line) and the confidence interval for the expected value represented as the grey band. Partial residuals are shown as dark grey dots. (c) Polynomial 4th order trend line relationship between number of days and capitulum length (mm) of *Lepas anatifera*. (d) Shows the expected value (blue line) and the confidence interval for the expected value represented as the grey band. Partial residuals are shown as dark grey dots.

Table 1
Drift time estimates of eight ghost nets found in the Maldives during the south west monsoon (SW, n = 5) and north east monsoon (NE, n = 3). Estimation were found by either measuring the capitulum length of the barnacle *Lepas anatifera* or by analysing the percentage cover of biofouling communities in image J. NA represents no data taken due to limitations in the field.

Net ID	Monsoon found	Capitulum length (mm)	Percentage biofouling cover (%)	Estimated drift time (days)
1	SW	NA	51	28 (± 2)
2	SW	NA	43	24 (± 1.5)
3	SW	NA	72	40 (± 2.5)
4	SW	NA	16.6	7.5 (± 1.5)
5	SW	NA	89	48 (± 3)
6	NE	5	NA	24 (± 2)
7	NE	26	NA	101 (± 10)
8	NE	18	NA	54 (± 2)

we did observe large clusters of *Amphora sp*. (identified as the same in Fig. 1b) present on net three, giving an independent indication that this net had been drifting for at least 28 days as inferred by our heatmap (Supplementary material S4) and diversity analyses. However, we observed no invertebrates present on any of our ghost nets which contradict the heatmap (Supplementary material S4). Following this methodology, we expected that ghost net five would have had invertebrates present, which it did not. This further highlight the variation in organism succession and the unreliability of using diversity indices or key taxa as markers to estimate age alone.

Particles were released at each of the eight ghost nets locations and backtracked according to age estimates above (Table 1, Supplementary material S5). Simulations for nets one, two (Fig. 5a) and four (Fig. 5b) suggest that they originated from inside the Exclusive Economic Zone (EEZ) of the Maldives. In contrast nets seven and eight (Table 1, Supplementary material S5) showed a comparatively wide dispersal of particles (Fig. 5b,c) with some drifting close to shorelines of Sri Lanka.

3.3. Putative origin for ghost nets without drift time estimates

At first look, simulations revealed a level of uncertainty with regards to a putative origin for the 326 ghost nets without drift time estimates. This is particularly true for long drift durations such as 120 days in this study. When modelling with the smallest drift time (10 days here), the simulated particles did not travel far outside the EEZ of the Maldives as indicated by high densities found well within the EEZ (Fig. 6a–b). The only fisheries operating in this area (that are reporting to the IOTC) are the Maldivian bait net fisheries (Fig. 6a–b). At 30 days of drift or more (Fig. 6c–j) the most likely origins fall outside of this zone and are therefore likely to be coming from other fisheries and EEZs from other countries. The results of the models obviously vary strongly depending on the season, indicating likely hot spots of net origin.

For the first 90 days during the NE monsoon, the model indicated that particles typically drift westerly. Numerous clusters accumulated well within the EEZ of the southern tip of India, Sri Lanka and the Maldives, very close to shore (Fig. 6a,c,e,g). After 90 days (Fig. 6i) it became increasingly difficult to determine a putative origin as particles were more dispersed. However, clusters continued to accumulate north of the Maldives within the EEZ of western India and to the east in Sri Lanka and eastern India. Interestingly, particles spread as far as Somalia, Yemen and Indonesia (Fig. 6g,i) but in lower densities. Comparatively, during the SW monsoon, particle clusters were much more defined, and a putative origin was more prominent in the open ocean of the Arabian Sea (Fig. 6b,f,h,j). Further, particles aggregated in higher densities when compared to the NE monsoon within the EEZ of Yemen, Oman, western India and western Sri Lanka (Fig. 6j).

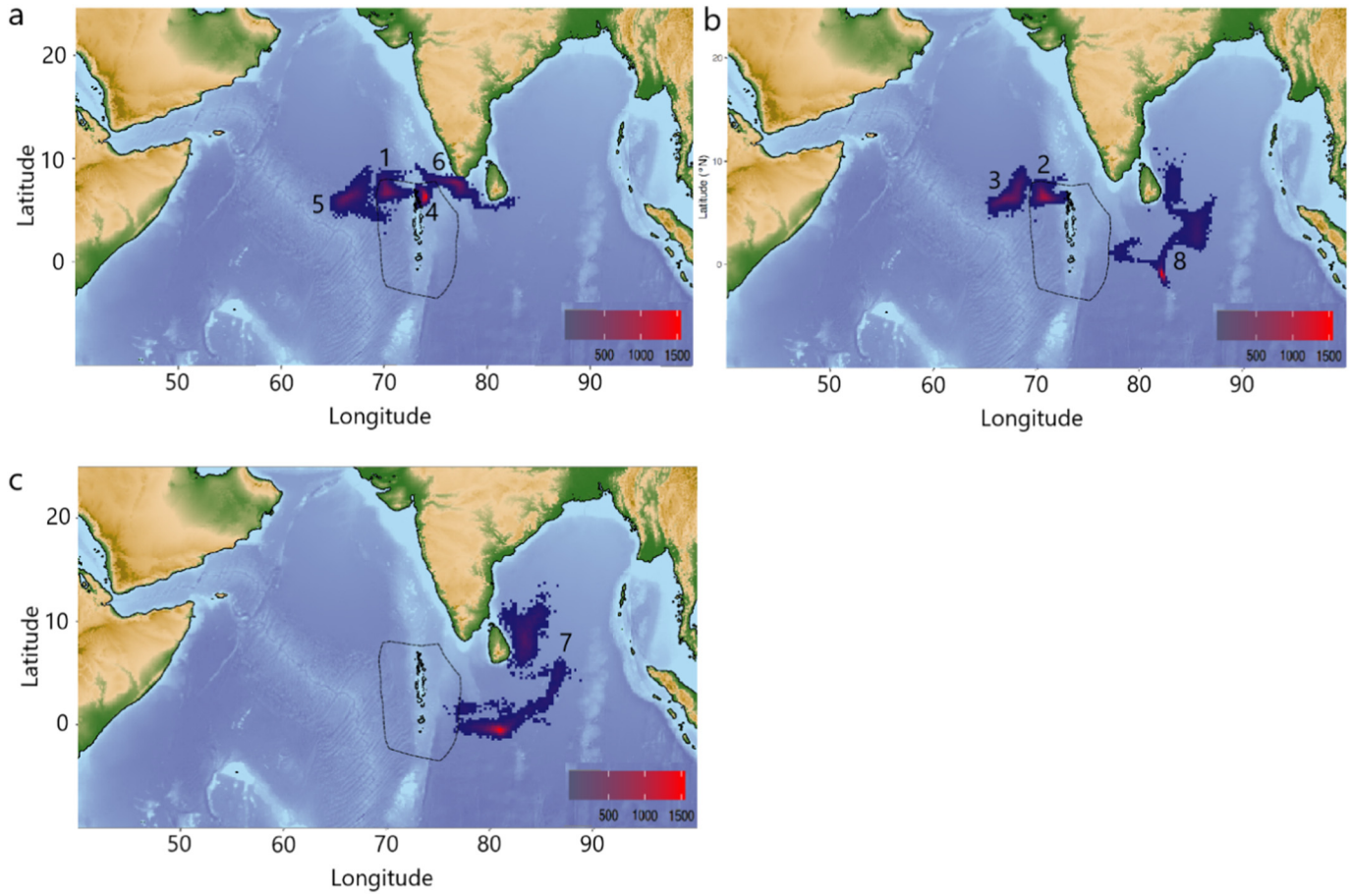

Fig. 5. Number of particles per 1/4° squares backtracked from each of the eight-net location and grouped to avoid overlapping (a) nets 5, 1, 4, and 6; (b) nets 3, 2, and 8; (c) net 7. Drift duration was set at the estimated drift times calculated for each net. Red areas indicate higher particle density. Maldivian exclusive economic zone (EEZ) is shown as black dotted line.

3.4. Possible fisheries responsible for ghost nets in the Maldives

For drift times longer than 10 days our simulations suggest that purse seine fisheries (Korea, Mauritius, Philippines, Spain, France and Seychelles) and gill nets from Sri Lanka are 'high risk' fisheries (with regard to possible source of lost nets). As these fisheries are active in areas where dense particle clusters occur, particularly at 90 days of drift across both seasons (Fig. 7a–d). In comparison, ring nets from Sri Lanka appear to be only a seasonal threat (Fig. 7e–f). However, the 'level' of threat from each country appears to vary depending on drift times. For example, nets that have been drifting for 60 days or less during the NE monsoon show a clear overlap in high density areas (red areas) where Sri Lankan purse seine fisheries operate. However, after this time, the dense clusters overlapped more with purse seine fisheries from flags of the EU (Spain and France), particularly after 90 days adrift (Fig. 7a–b, Supplementary material S6). As drift time increases beyond 90 days to 120 days, particles become more dispersed, making it much more difficult to assign high risk fisheries in the area. Comparatively the SW monsoon simulations provide a clearer putative origin for all drift times analysed in this study. Here the dense clusters of particles push north into the Arabian Sea as drift time increases. For the first 30 days the only major concern is from gill nets operated by Sri Lanka. At 60 days purse seiners from Spain and the Seychelles begin to overlap with these areas of high density and by 120 days purse seine fisheries from Mauritius, Korea, and Seychelles join the ranks of Spain and France (Supplementary material S7).

It should be noted that Japanese purse seine vessels are also shown to be fishing in areas where high particle density occurs during the NE monsoon. However, a large number of Japanese coordinates appeared on land when we mapped them. This is obviously an error on the reporting and therefore based on this level of uncertainty we had to exclude Japanese purse seine fisheries from our analyses.

4. Discussion

The aging of abandoned, lost or discarded fishing gear (ALDFG), more specifically 'ghost nets', is possible, at least to some degree. Percentage cover of biofouling communities and the capitulum size of the goosenecked barnacle, *Lepas anatifera* appeared as the most reliable methods in order to determine minimum drift times due to the low variability between replicates and clear trends in overall measurement. Succession of diatom communities and arrival of rare and macrofouling organisms may also provide additional information that compliments such estimations. The Lagrangian particle dispersal simulation shows the possibility of wide spatial origin of particles (i.e., ghost nets here), arriving in the Maldivian EEZ yet defines likely hotspots for putative origins of a given net. Overlapping spatial distribution of fisheries over these simulations allows the identification of fisheries that are most likely to contribute to the ghost nets found in the Maldivian EEZ.

4.1. Biofouling communities and ghost gear aging

Fishing nets provide a novel and niche habitat for a wide diversity of fouling organisms (Reisser et al., 2014; Fazey and Ryan, 2016; Kooi et al., 2017). Here, we illustrate that a relatively high diversity of diatoms arrives in the first few days. This is followed by a number of

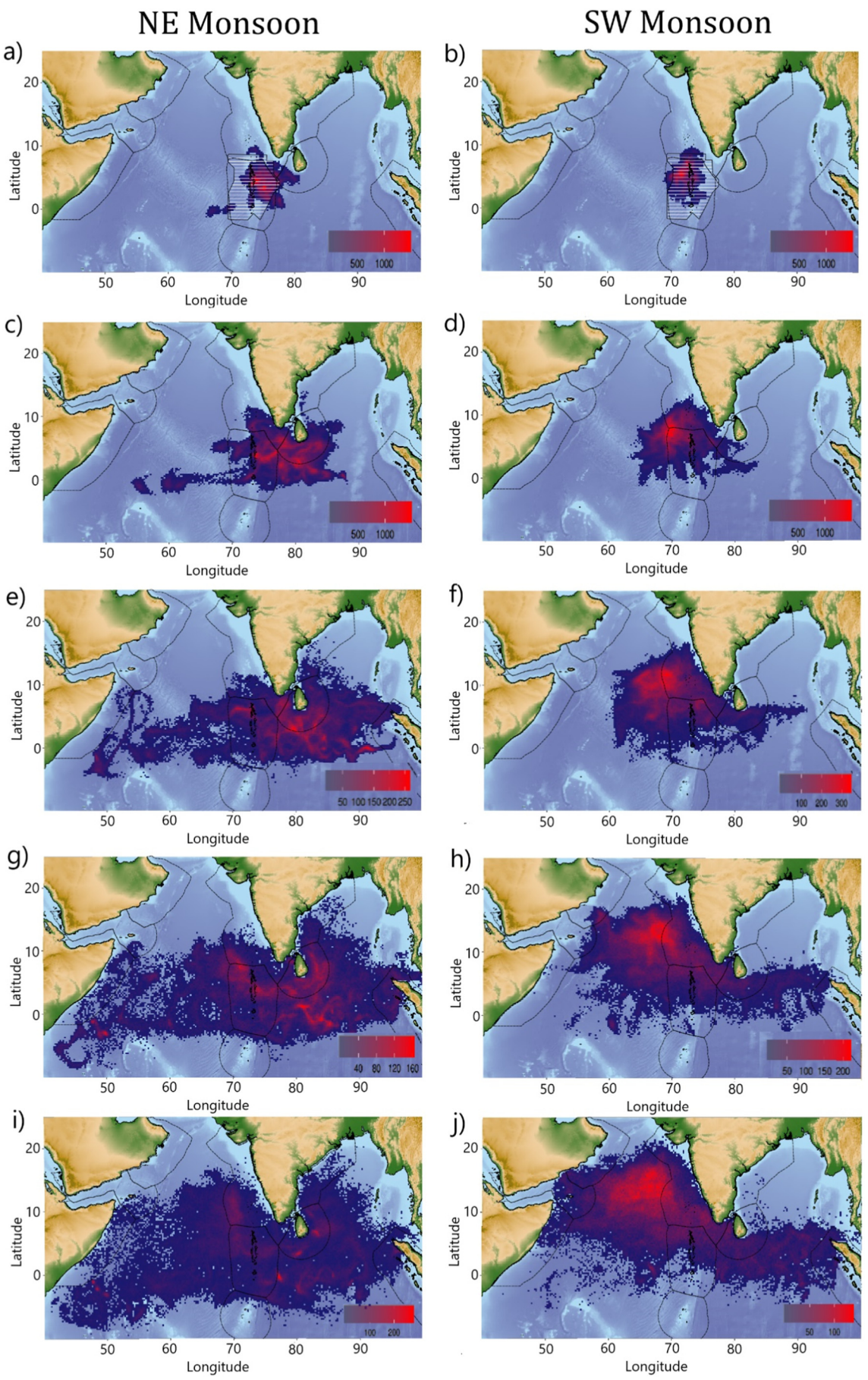

(caption on next page)

Fig. 6. Number of particles per 1/4° squares backtracked from the location and time of the 326 ghost nets collected during the NE monsoon (n = 149, left) and SW monsoon (n = 177, right). As there was no drift time estimates for these nets drift periods of 10 (a–b), 30 (c–d), 60 (e–f), 90 (g–h) and 120 days (i–j) were used. Red areas indicate higher particle density. Exclusive economic zones (EEZ) are shown as black dotted line for each surrounding country. Maldivian bait fishery area of operation highlighted as white horizontal lines (a–b).

other unidentified organisms including bacteria and invertebrates. Collectively, this is known as the 'plastisphere' (Zettler et al., 2013). It is reasonable to assume that this plastisphere may be the initial driver that attracts larger predators such as sea turtles to ghost nets in search of food. Interestingly, we found that bacteria quickly colonise the plastic surface and eventually flourish to become the most abundant organisms. It has previously been shown that these bacteria impact the surface of floating plastic, forming pits and groves as a result of biodegradation (Artham et al., 2009; Reisser et al., 2014). This may mean that the bacteria are directly influencing the breakdown of ghost nets.

Percentage cover of biofouling organisms on the experimental nets show a characteristic sigmoidal curve (Fig. 3f), in a similar pattern to the biofouling which occurs on marine glass samples in Europe (Lehaitre et al., 2008). Moreover, our largest barnacle found on the

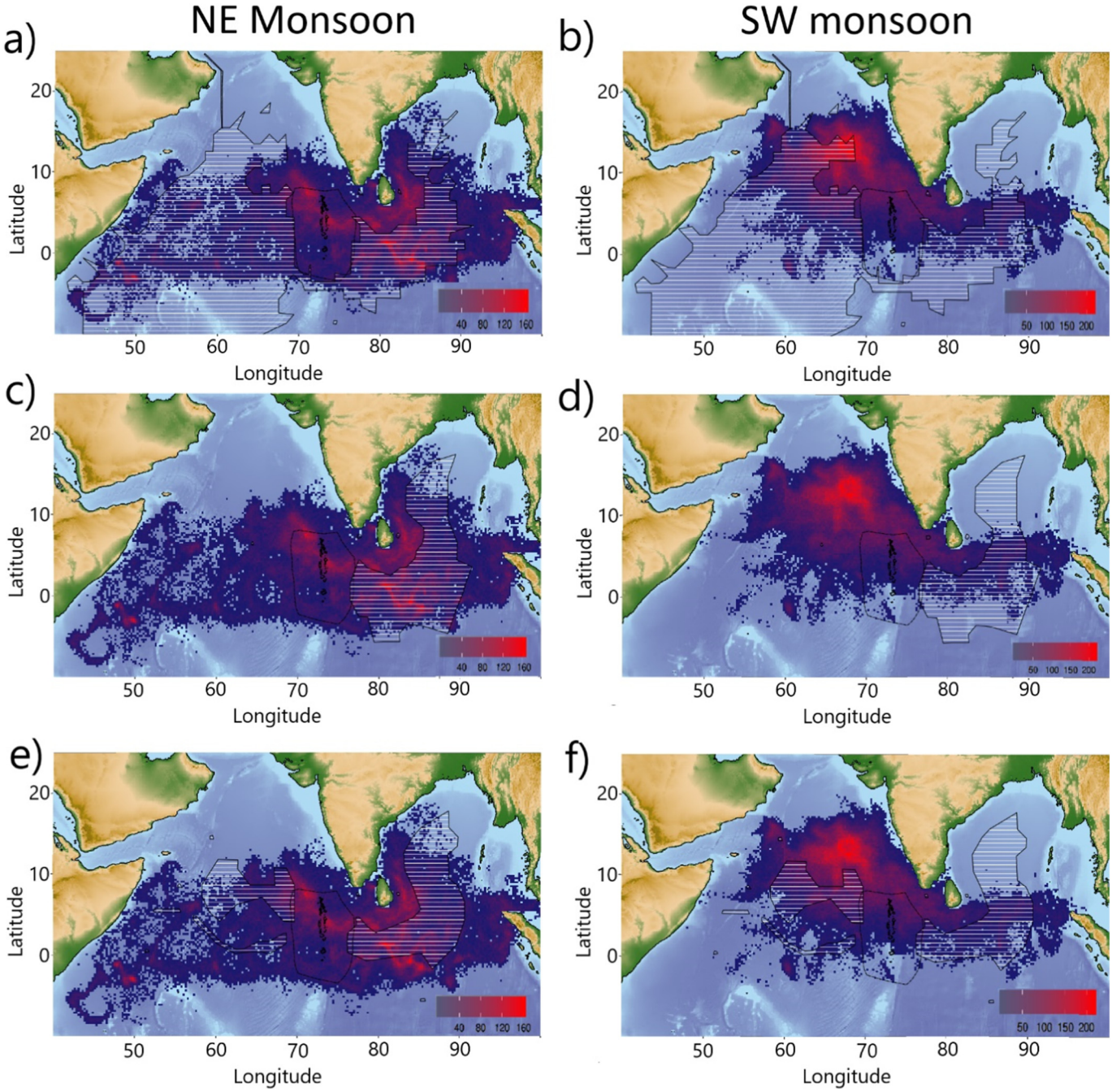

Fig. 7. Number of particles per 1/4° squares backtracked from the collected ghost net locations after 90 days of drift during the NE monsoon (left) and SW monsoon (right). Red areas indicate higher particle density. Maldivian exclusive economic zone (EEZ) is shown as black dotted line. Spatial distribution of purse seine fisheries (shown in white shaded area) operating from Sri Lanka, Philippine, Korea, Spain, France, Mauritius and the Seychelles (a–b), Ring net fisheries from Sri Lanka (c–d) and Gill net fisheries from Sri Lanka (e–f).

ghost nets (27.9 mm) was of a similar size to that reported previously (25 mm, Evans, 1958). Further, our age estimates and those from this latter paper were similar (101 and 107 days respectively). These latter studies were undertaken in countries other than the Maldives (and the wider Indo-Pacific) indicating that our tools for estimating drift time may well have global reach.

Aging drift times had the highest confidence up to the first 100 days in the water. Percentage cover of biofouling communities becomes largely unusable after 56 days. However, capitulum size of *L. anatifera* tracked well up to 105 days and possibly expands past this time point as the barnacles in this study had not reached their known maximum growth size (De Wolf, 2008). Capitulum size in excess of 50 mm has been reported for this species (Magni et al., 2015), therefore it is unlikely that maximum size was reached in this study. It is however important to recognise (as stated previously), that surface roughness and topography play important factors in bioaccumulation and growth rates (Scheuerman et al., 1998). Twisted nets are typical of net types found in the Maldives (Stelfox et al., 2015, 2019). Future analyses should focus on rates of growth on monofilament and braided nets to compare similarities and differences in bioaccumulation rates and diversity. Additionally, minimum drift time analyses are based on growth rates in coastal environments on fixed objects. This was undertaken for obvious practical and ethical reasons. That said, it should be noted that free-floating ghost nets may well be subject to spatial fluctuations in environmental conditions that may impact biofouling organisms and their succession (Sudhakar et al., 2007).

4.2. Lagrangian simulations

Including diffusion in Lagrangian simulations, backwards in time, is a valuable approach to obtain probability distributions of past positions (Batchelder, 2006). At least in the context of either limited spatial (here 1/3°) or temporal (here 5 days) resolutions of the forcing current product (here OSCAR). Despite their coarse resolution, current products based on remote sensing data, like OSCAR, have been shown to simulate surface drift trajectories satisfactorily (Hart-Davis et al., 2018, using GlobCurrent) with similar (or even higher) accuracies than higher-resolution oceanographic model outputs (Scott et al., 2012, using Surcouf). Using OSCAR, Davies et al. (2017) showed that simulated trajectories of fish aggregating devices (FADs) were generally consistent with observations. However, in the Indian Ocean OSCAR velocities were shown to be generally lower than velocities derived from oceanographic drift trajectories (Imzilen et al., 2019). That said, the zonal component of OSCAR velocities appears to be more accurate than the meridional component (Sikhakolli et al., 2013).

4.3. Fishery interaction

The youngest ghost net analysed in this study (estimated at drifting for only 7.5 days) along with nets one and two (28 and 24 days respectively), suggests an original source origin from inside the EEZ of the Maldives. However, the relatively large mesh size associated with these nets is untypical of those usually used as bait nets in this area, suggesting the possibility of illegal, unreported, and/or unregulated fishing practices taking place within the Maldives. Comparatively, ghost net seven (Fig. 5c), found during the NE monsoon, was the longest drifter at around 101 days. Multiple clusters were simulated overlapping a wide variety of fisheries including gill and ring nets from Sri Lanka and purse seine fisheries from Spain, France, Seychelles and Korea.

Fisheries operating in the area of study are widespread (IOTC, 2018) and those labelled as 'high-risk' fisheries (with regard to likely contributors of the majority of nets) fluctuate depending on spatial distribution, season and estimated drift times. However, gill nets from Sri Lanka appear to be high risk fisheries regardless of season at all drift times longer than 30 days. Additionally, the wide dispersal of particles (nets) for the longer modelled drift times (approaching 120 days, Fig. 6), coupled with the invasion of multiple EEZs particularly close to shorelines of Sri Lanka and India (Fig. 6) suggests that an unconfirmed proportion of ghost nets entering the Maldives could be from a variety of small scale artisanal fisheries. This is further supported by observations of fragments of ghost nets drifting into the Maldives with Indian markings on floatation devices (Stelfox et al., 2015). Although purse seine nets appear to be problematic across both seasons (Fig. 7a–b), there are temporal changes that influence the risk that specific countries pose. Here, the Sri Lankan purse seine fisheries pose significant risks at all drift times during the NE monsoon, but this is reduced during the SW monsoon. Comparatively, when drift times are > 60 days during the NE monsoon, purse seine fisheries from France and Spain are the only additional high-risk fisheries analysed in this study during this period (Supplementary material S6). Interestingly, if a net is drifting for only 30 days during the SW monsoon, it is unlikely to be originating from these fisheries. However, if the nets drift for longer periods, fisheries associated with Spain and the Seychelles increase in their likelihood of being the origin of the nets. Korea, Mauritius and France also 'come into play' as likely sources when the drift is past 90 days (Supplementary material S7). Evidence to support the modelling and implicating purse seine fisheries in the origin of a proportion of nets found floating in the Maldives comes from the stranding of FADs (Stelfox et al., 2015, 2019). Identifying ghost nets to a specific fishery and/or location can, however, be challenging, as more often than not the gear is unmarked (Stelfox et al., 2015). In the Maldives it is thought that many of the ghost nets that drift into the EEZ originate from neighbouring countries (Stelfox et al., 2015), and our Lagrangian simulations support this hypothesis. However, spatial distribution data from major fisheries such as India, Pakistan, Oman and Yemen and those from coastal fisheries from all surrounding countries (which dominate the Indian Ocean) are sparse and, in some cases, completely absent in the IOTC database (IOTC, 2018). This lack of reporting means that although our analysis is as thorough as possible, we may still be overlooking the risk of the fisheries associated with these countries (where no spatial distribution data is available).

4.4. Future recommendations

A lack of data on gear types and spatial distributions of small and large-scale fisheries means it remains difficult to accurately identify responsible fisheries in the Indian Ocean. The IOTC working party on data collection and statistics note this to be the case especially for artisanal fisheries and in particular for gill nets (IOTC, 2018). A cross sector collaboration between governments, NGOs, IGOs and the private sector should take precedent, aimed at improving the collection and transparency of such data and share resources where possible. Simulations and age estimates (combined) highlight that purse seine fisheries and gill nets are likely key candidates for a major part of the ghost gear found drifting into the EEZ of the Maldives. To minimise damage to sensitive habitats in this country, a recovery project (similar to "FAD watch" set up in the Seychelles; Zudaire et al., 2018) could be initiated throughout the Maldives. Such a project would require the collaboration of Maldivian NGOs, the government and purse seine fisheries from the EU (Spain and France), Mauritius, the Seychelles and Korea. In the Seychelles, FAD watch allows for the recovery of FADs that come within 3–5 nautical miles of selected islands in the Seychelles. Through this project a 20% and 41% reduction in beaching events have been observed in 2016 and 2017, respectively.

It should also be noted that for the modelling, we assumed ghost nets behave like particles and we do not include net geometry and/or vertical profile or the impact of stokes drift into account (Dobler et al. 2019). Future analyses of ghost net drifts should focus on how bioaccumulation may impact floating times and vertical profile and how ghost net geometry may influence drifting trajectories. Although diversity indices were not effective in estimating age in this study, different species of diatoms and other macrofoulers can provide additional

tools to help estimate drift times. Categorising bioaccumulation composition for different regions may help identify region specific organisms that could give additional clues towards drift trajectories and ghost gear origins. Finally, we only report diatoms that could be visually identified, future analyses of fouling communities should focus on utilising molecular tools to increase the known diversity at any given time point.

To conclude, here in this study we illustrate that percentage biofouling cover and capitulum length of the gooseneck baranacle, *Lepas anatifera* can be used to infer minimum drift times of ghost gear. We show that nets in the Maldives have a minimum drift times from as little as 7.5 days to over 101. Our back-track modelling suggests that nets with shorter drift times (< 30 days) likely originate from illegal, unreported and unregulated fishing which is occurring within the Maldives EEZ. While those drifting for longer than 30 days appear to be originating from purse seine and gill nets fisheries (from a number of countries), along with smaller scale artisanal fisheries in areas such as Sri Lanka.

CRediT authorship contribution statement

Martin Stelfox: Conceptualization, Methodology, Writing - original draft, Software, Formal analysis, Investigation. **Christophe Lett:** Software, Formal analysis, Writing - review & editing. **Geraldine Reid:** Resources, Writing - review & editing. **Graham Souch:** Resources, Writing - original draft. **Michael Sweet:** Conceptualization, Methodology, Resources, Writing - original draft, review & editing.

Declaration of competing interest

The authors declare that they have no known competing financial interests or personal relationships that could have appeared to influence the work reported in this paper.

Acknowledgements

We are grateful to all the volunteers of the Olive Ridley Project for collecting and reporting ghost gear in the Maldives and wider Indian Ocean. We thank Jenni Choma, Sonia Valladares, Claire Nerissa, Claire Petros, Deborah Burn and Josie Chandler for assisting with experimental deployment and data collection. We would also like to extend our gratitude to Coco Palm Dhuni Kolhu Resort, Baa atoll and Bodu Hithi resort, North Male atoll for allowing net experiments in their lagoons. Thank you to the team at SureScreen Scientifics, particularly Troy Whyte and Arthur Green for the use of the SEM. Thank you to Gareware Wall Ropes Ltd. for supplying new nets for bioaccumulation analyses.

Appendix A. Supplementary data

Supplementary data to this article can be found online at https://doi.org/10.1016/j.marpolbul.2020.111037.

References

Adam, M.S., 2006. Country review: Maldives. Review of the state of world marine capture fisheries management: Indian Ocean. FAO Fish. Tech. Pap. 488, 383–392.
Adam, M.S., Jauharee, A.R., Miller, K.I., 2015. Review of yellowfin tuna fisheries in the Maldives. In: Paper Submitted to IOTC Working Party on Tropical Tunas (IOTC-2015-WPTT-17-17).
Alonso-Garcia, M., Rodrigues, T., Abrantes, F., Padilha, M., Alvarez-Zarikian, C.A., Kunkelova, T., Wright, J.D., Betzler, C., 2019. Sea-surface temperature, productivity and hydrological changes in the Northern Indian Ocean (Maldives) during the interval~ 575-175 ka (MIS 14 to 7). Palaeogeogr. Palaeoclimatol. Palaeoecol. 536, 109376.
Artham, T., Sudhakar, M., Venkatesan, R., Nair, C.M., Murty, K.V.G.K., Doble, M., 2009. Biofouling and stability of synthetic polymers in sea water. Int. Biodeterior. Biodegradation 63, 884–890.
Banerjee, I., Pangule, R.C., Kane, R.S., 2011. Antifouling coatings: recent developments in the design of surfaces that prevent fouling by proteins, bacteria, and marine organisms. Adv. Mater. 23, 690–718.
Batchelder, H.P., 2006. Forward-in-time-/backward-in-time-trajectory (FITT/BITT) modeling of particles and organisms in the coastal ocean. J. Atmos. Ocean. Technol. 23, 727–741. https://doi.org/10.1175/JTECH1874.1.
Callow, J.A., Callow, M.E., 2011. Trends in the development of environmentally friendly fouling-resistant marine coatings. Nat. Commun. 2, 244.
Consoli, P., Falautano, M., Sinopoli, M., Perzia, P., Canese, S., Esposito, V., Battaglia, P., Romeo, T., Andaloro, F., Galgani, F., Castriota, L., 2018. Composition and abundance of benthic marine litter in a coastal area of the central Mediterranean Sea. Mar. Pollut. Bull. 136, 243–247.
Davies, T., Curnick, D., Barde, J., Chassot, E., 2017. Potential environmental impacts caused by beaching of drifting fish aggregating devices and identification of management solutions and uncertainties. In: First IOTC Ad Hoc Working Group on FADs, at Madrid, Spain, Volume: IOTC-2017-WGFAD01-08 Rev_1, . http://horizon.documentation.ird.fr/exl-doc/pleins_textes/divers18-02/010071786.pdf.
De Wolf, P., 2008. Very large goose-barnacles, Lepas anatifera L., 1758 (Cirripedia, Thoracica). Crustaceana 81, 637–639.
Dobler, D., Huck, T., Maes, C., Grima, N., Blanke, B., Martinez, E., Ardhuin, F., 2019. Large impact of Stokes drift on the fate of surface floating debris in the South Indian Basin. Mar. pollut. bull. 148, 202–209.
Evans, F., 1958. Growth and maturity of the barnacles Lepas hillii and Lepas anatifera. Nature 182, 1245.
Fazey, F.M., Ryan, P.G., 2016. Biofouling on buoyant marine plastics: an experimental study into the effect of size on surface longevity. Environ. Pollut. 210, 354–360.
Fritz, H.M., Synolakis, C.E., McAdoo, B.G., 2006. Maldives field survey after the December 2004 Indian Ocean tsunami. Earthquake Spectra 22, 137–154.
Guerrini, F., Mari, L., Casagrandi, R., 2019. Modelling plastics exposure for the marine biota: risk maps for fin whales in the Pelagos Sanctuary (North-Western Mediterranean). Front. Mar. Sci. 6, 299.
Hardesty, B.D., Good, T.P., Wilcox, C., 2015. Novel methods, new results and science-based solutions to tackle marine debris impacts on wildlife. Ocean & Coastal Management 115, 4–9.
Hart-Davis, M.G., Backeberg, B.C., Halo, I., van Sebille, E., Johannessen, J.A., 2018. Assessing the accuracy of satellite derived ocean currents by comparing observed and virtual buoys in the Greater Agulhas Region. Remote Sens. Environ. 216, 735–746.
Hellio, C., Marechal, J.P., Veron, B., Bremer, G., Clare, A.S., Le Gal, Y., 2004. Seasonal variation of antifouling activities of marine algae from the Brittany coast (France). Mar. Biotechnol. 6, 67–82.
Imzilen, T., Chassot, E., Barde, J., Demarcq, H., Maufroy, A., Roa-Pascuali, L., Ternon, J.F., Lett, C., 2019. Fish aggregating devices drift like oceanographic drifters in the near-surface currents of the Atlantic and Indian Oceans. Prog. Oceanogr. 171, 108–127.
IOTC, 2018. Datasets-CEAll. https://www.iotc.org/documents/WPTmT/07/DP/DATA/07-CEALL.
IOTC–WPDCS14, 2018. Report of the 14th Session of the IOTC Working Party on Data Collection and Statistics. Victoria, Seychelles, 29 November-1 December 2018. IOTC–2018–WPDCS14–R[E]. pp. 71.
Jalón-Rojas, I., Wang, X.H., Fredj, E., 2019. A 3D numerical model to track marine plastic debris (TrackMPD): sensitivity of microplastic trajectories and fates to particle dynamical properties and physical processes. Mar. Pollut. Bull. 141, 256–272.
Kiessling, T., Gutow, L., Thiel, M., 2015. Marine litter as habitat and dispersal vector. In: Marine Anthropogenic Litter. Springer, Cham, pp. 141–181.
Kooi, M., Nes, E.H.V., Scheffer, M., Koelmans, A.A., 2017. Ups and downs in the ocean: effects of biofouling on vertical transport of microplastics. Environmental science & technology 51, 7963–7971.
Kruskal, W.H., Wallis, W.A., 1952. Use of ranks in one-criterion variance analysis. J. Am. Stat. Assoc. 47, 583–621.
Lagerloef, G.S.E., Mitchum, G.T., Lukas, R.B., Niiler, P.P., 1999. Tropical Pacific near-surface currents estimated from altimeter, wind, and drifter data. J. Geophys. Res. 104, 23313–23326. https://doi.org/10.1029/1999JC900197.
Lebreton, L.M., Greer, S.D., Borrero, J.C., 2012. Numerical modelling of floating debris in the world's oceans. Mar. Pollut. Bull. 64, 653–661.
Lehaitre, M., Delauney, L., Compère, C., 2008. Biofouling and underwater measurements. Real-time observation systems for ecosystem dynamics and harmful algal blooms: theory, instrumentation and modelling. In: Oceanographic Methodology Series. UNESCO, Paris, pp. 463–493.
Lett, C., Verley, P., Mullon, C., Parada, C., Brochier, T., Penven, P., Blanke, B., 2008. A Lagrangian tool for modelling ichthyoplankton dynamics. Environ. Model Softw. 23, 1210–1214. https://doi.org/10.1016/j.envsoft.2008.02.005.
Liubartseva, S., Coppini, G., Lecci, R., Creti, S., 2016. Regional approach to modeling the transport of floating plastic debris in the Adriatic Sea. Mar. Pollut. Bull. 103, 115–127.
Magni, P.A., Venn, C., Aquila, I., Pepe, F., Ricci, P., Di Nunzio, C., Ausania, F., Dadour, I.R., 2015. Evaluation of the floating time of a corpse found in a marine environment using the barnacle *Lepas anatifera* L.(Crustacea: Cirripedia: Pedunculata). Forensic Sci. Int. 247, 6–e10.
Matsuoka, T., Nakashima, T., Nagasawa, N., 2005. A review of ghost fishing: scientific approaches to evaluation and solutions. Fish. Sci. 71, 691–702.
Maximenko, N., Hafner, J., Niiler, P., 2012. Pathways of marine debris derived from trajectories of Lagrangian drifters. Mar. Pollut. Bull. 65, 51–62.
Miller, M., Steele, C., Horn, D., Hanna, C., 2018. Marine debris trends: 30 years of change on Ventura County and Channel Island beaches. Western North American Naturalist 78, 328–341.

Nall, C.R., Schläppy, M.L., Guerin, A.J., 2017. Characterisation of the biofouling community on a floating wave energy device. Biofouling 33, 379–396.
Peliz, A., Marchesiello, P., Dubert, J., Marta-Almeida, M., Roy, C., Queiroga, H., 2007. A study of crab larvae dispersal on the Western Iberian Shelf: physical processes. J. Mar. Syst. 68, 215–236.
Pielou, E.C., 1966. The measurement of diversity in different types of biological collections. J. Theor. Biol. 13, 131–144.
Rajagopal, S., Jenner, H.A., 2012. Biofouling in cooling water intake systems: ecological aspects. In: Operational and Environmental Consequences of Large Industrial Cooling Water Systems. Springer, Boston, MA, pp. 13–32.
Reisser, J., Shaw, J., Hallegraeff, G., Proietti, M., Barnes, D.K., Thums, M., Wilcox, C., Hardesty, B.D., Pattiaratchi, C., 2014. Millimeter-sized marine plastics: a new pelagic habitat for microorganisms and invertebrates. PLoS One 9 (6).
Core Team, R., 2018. R: A Language and Environment for Statistical Computing. R Foundation for Statistical Computing Vienna. https://www.R-project.org.
Saldanha, H.J., Sancho, G., Santos, M.N., Puente, E., Gaspar, M.B., Bilbao, A., Monteiro, C.C., Gomez, E., Arregi, L., 2003. The use of biofouling for ageing lost nets: a case study. Fish. Res. 64, 141–150.
Scheuerman, T.R., Camper, A.K., Hamilton, M.A., 1998. Effects of substratum topography on bacterial adhesion. J. of Colloid and Interface Science 208, 23–33.
Schneider, C.A., Rasband, W.S., Eliceiri, K.W., 2012. NIH image to ImageJ: 25 years of image analysis. Nat. Methods 9, 671–675.
Schott, F.A., Xie, S.P., McCreary Jr., J.P., 2009. Indian Ocean circulation and climate variability. Rev. Geophys. 47 (1).
Schultz, M.P., 2007. Effects of coating roughness and biofouling on ship resistance and powering. Biofouling 23, 331–341.
Scott, R.B., Ferry, N., Drévillon, M., Barron, C.N., Jourdain, N.C., Lellouche, J.-M., Metzger, E.J., Rio, M.-H., Smedstad, O.M., 2012. Estimates of surface drifter trajectories in the equatorial Atlantic: a multi-model ensemble approach. Ocean Dyn. 62, 1091–1109. https://doi.org/10.1007/s10236-012-0548-2.
Shankar, D., Vinayachandran, P.N., Unnikrishnan, A.S., 2002. The monsoon currents in the north Indian Ocean. Prog. Oceanogr. 52, 63–120.
Shapiro, S.S., Wilk, M.B., 1972. An analysis of variance test for the exponential distribution (complete samples). Technometrics 14, 355–370.
Shi, W., Park, H.C., Baek, J.H., Kim, C.W., Kim, Y.C., Shin, H.K., 2012. Study on the marine growth effect on the dynamic response of offshore wind turbines. Int. J. Precis. Eng. Manuf. 13, 1167–1176.
Sikhakolli, R., Sharma, R., Basu, S., Gohil, B.S., Sarkar, A., Prasad, K.V.S.R., 2013. Evaluation of OSCAR ocean surface current product in the tropical Indian Ocean using in situ data. J Earth Syst Sci 122, 187–199. https://doi.org/10.1007/s12040-012-0258-7.
Simpson, E.H., 1949. Measurement of diversity. nature 163, 688.
Stelfox, M., Hudgins, J., Sweet, M., 2016. A review of ghost gear entanglement amongst marine mammals, reptiles and elasmobranchs. Mar. Pollut. Bull. 111, 6–17.
Stelfox, M., Bulling, M., Sweet, M., 2019. Untangling the origin of ghost gear within the Maldivian archipelago and its impact on olive ridley (Lepidochelys olivacea) populations. Endanger. Species Res. 40, 309–320.
Stelfox, M.R., Hudgins, J.A., Ali, K., Anderson, R.C., 2015. High mortality of olive ridley turtles (Lepidochelys olivacea) in ghost nets in the central Indian Ocean. BOBLME-2015-Ecology 14, 1–23.
Sudhakar, M., Trishul, A., Doble, M., Kumar, K.S., Jahan, S.S., Inbakandan, D., Viduthalai, R.R., Umadevi, V.R., Murthy, P.S., Venkatesan, R., 2007. Biofouling and biodegradation of polyolefins in ocean waters. Polym. Degrad. Stab. 92, 1743–1752.
Von Brandt, A., 1984. Fish Catching Methods of the World, 3rd edn. Fishing News Books Ltd, Farnham.
Warnes, G.R., Bolker, B., Bonebakker, L., Gentleman, R., Liaw, W.H.A., Lumley, T., Maechler, M., Magnusson, A., Moeller, S., Schwartz, M., Venables, B., 2015. gplots: various R programming tools for plotting data. The comprehensive R archive network. Available. http://CRAN.R-project.org/package=gplots.
Watters, D.L., Yoklavich, M.M., Love, M.S., Schroeder, D.M., 2010. Assessing marine debris in deep seafloor habitats off California. Mar. Pollut. Bull. 60, 131–138.
Weaver, W., Shannon, C.E., 1949. The mathematical theory of communication. University of Illinois. Urbana 13, 1–138.
Wilcox, C., Hardesty, B.D., Sharples, R., Griffin, D.A., Lawson, T.J., Gunn, R., 2013. Ghostnet impacts on globally threatened turtles, a spatial risk analysis for northern Australia. Conserv. Lett. 6, 247–254.
Wilcox, C., Mallos, N.J., Leonard, G.H., Rodriguez, A., Hardesty, B.D., 2016. Using expert elicitation to estimate the impacts of plastic pollution on marine wildlife. Mar. Policy 65, 107–114.
Wood, S., Baums, I.B., Paris, C.B., Ridgwell, A., Kessler, W.S., Hendy, E.J., 2016. El Niño and coral larval dispersal across the eastern Pacific marine barrier. Nat. Commun. 7, 12571.
Ye, S., Andrady, A.L., 1991. Fouling of floating plastic debris under Biscayne Bay exposure conditions. Mar. Pollut. Bull. 22, 608–613.
Zettler, E.R., Mincer, T.J., Amaral-Zettler, L.A., 2013. Life in the “plastisphere”: microbial communities on plastic marine debris. Environmental science & technology 47, 7137–7146.
Zudaire, I., Santiago, J., Grande, M., Murua, H., Adam, P.A., Nogués, P., Collier, T., Morgan, M., Khan, N., Baguette, F., Morón, J., 2018. FAD Watch: a collaborative initiative to minimize the impact of FADs in coastal ecosystems. In: A Paper Submitted to the 14th IOTC Working Party on Ecosystems and Bycatch, Cape Town, South Africa.